ChemComm

Accepted Manuscript

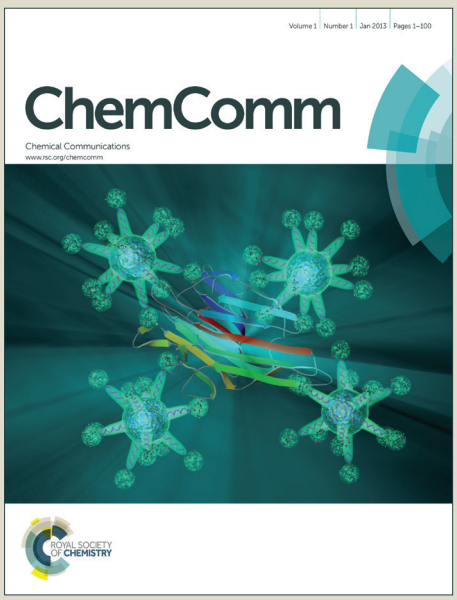

ROYAL SOCIETY OF CHEMISTRY

www.rsc.org/chemcomm

Journal Name

RSCPublishing

COMMUNICATION

Smart dual-functional warhead for folate receptor-specific activatable imaging and photodynamic therapy

Cite this: DOI: 10.1039/x0xx00000x

Jisu Kim[a], Ching-Hsuan Tung[b] and Yongdoo Choi*[a]

Received 00th January 2012,
Accepted 00th January 2012

DOI: 10.1039/x0xx00000x

www.rsc.org/

Smart dual-targeted theranostic agent becomes highly fluorescent and phototoxic only when its linker is cleaved by tumor-associated lysosomal enzyme cathepsin B after internalization into folate receptor-positive cancer cells.

Using combinations of chemical photosensitizers and light, photodynamic therapy (PDT) has been successfully used to treat cancers and other nonmalignant conditions.[1] Typical photosensitizers are non-toxic to cells in the absence of light, but they become highly cytotoxic in the presence of light by converting surrounding oxygen molecules ($^3O_2$) into reactive singlet oxygen molecules ($^1O_2$), thereby selectively damaging tumor tissues *in situ*. Despite the significant advantages of PDT over conventional chemotherapy, the clinical applications of PDT have limitations such as limited tumor selectivity and the unfavorable biodistribution of conventional PDT agents.[2] In particular, the nonspecific activation of both fluorescence emission and singlet oxygen generation (SOG) in normal tissues results in poor imaging contrast and sunlight-induced skin phototoxicity, thereby limiting their utility as theranostic agents.

To overcome such drawbacks, targeted PDT agents have been developed with enhanced specificity and improved photosensitizer delivery.[3,4] However, most targeted PDT agents are "always on." Consequently, these agents have the potential problem of high background fluorescence when circulating in the blood stream, which can result in a low target-to-background ratio in *in vivo* imaging. Additionally, although the receptors targeted by these PDT agents are overexpressed in tumor cells, they are also located in healthy cells, which greatly outnumber the tumor cells.[5] Therefore, non-specific uptake by non-targeted cells and surrounding normal cells can cause unwanted phototoxic effects and further decrease the target-to-background signal ratio. Therefore, dual-targeted theranostic agents that not only have high target-cancer cell specificity but also only "turn on" their fluorescence and SOG once they are inside the target cells are greatly needed. However, their development has been very challenging.

Here, we show that the development of small-sized, dual-targeted, and activatable theranostic agents could be achieved through the conjugation of folic acid (FA) with photosensitizers *via* chemical linkers, which become cleavable within viable cancer cells (Fig. 1A).

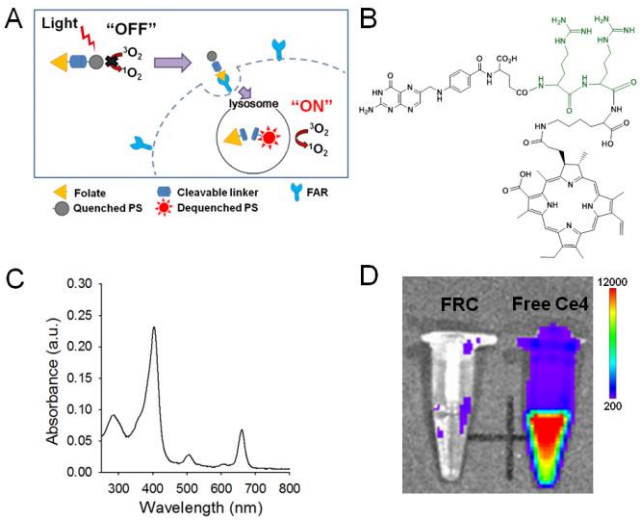

Fig. 1 a) Schematic diagram of the cleavable folate-photosensitizer (PS) conjugate for dual-targeted and activatable NIR fluorescence imaging and photodynamic therapy. Fluorescence emission and SOG of the PS conjugate were quenched in the extracellular environment. After internalization into FAR-positive viable cancer cells, linkers in the conjugates were cleaved by tumor-associated lysosomal enzymes, activating fluorescence and SOG of the PS conjugate. b) The chemical structure of FAR-targeting and cathepsin B-activatable FRC conjugates. c) UV-Vis absorption spectrum of FRC conjugate. d) NIR fluorescence image of FRC conjugate and free Ce4 solutions. Photosensitizers were dissolved in PBS solutions at a concentration of 1 μM and the NIR fluorescence image ($\lambda_{ex.}$ 660 ± 10 nm, $\lambda_{em.}$ 710 nm ± 20 nm) was obtained with a fluorescence imaging system (IVIS Lumina XR).

The folic acid receptor (FAR) is a naturally occurring 38-kDa glycol polypeptide that is overexpressed in many types of cancers.[6] FAR binds FA with a high affinity. Therefore, FA has long been used as a targeting ligand to deliver various payloads to FAR-expressing tumors and inflamed cells. In addition to conventional understanding of its targeting capability, we found that it could also act as an excellent shade, masking fluorescence and phototoxicity of the adjacent photosensitizers. We hypothesized that, in the conjugate's native state, the photosensitizers are within close proximity to FA, and both near-infrared (NIR) fluorescence emission

and SOG of the photosensitizers are quenched (OFF). However, when the conjugates specifically bind to FAR (first target) and become internalized *via* receptor-mediated endocytosis into FAR-overexpressing cancer cells, the chemical linkers in the conjugates are cleaved by a cancer-selective enzyme (second target), causing the release of the photosensitizers from FA. This results in the complete recovery (ON) of fluorescence and SOG of the photosensitizer inside target cancer cells. As a proof of principle of this approach, we synthesized a conjugate, termed FRC, of FA and chlorin e4 (Ce4) with a short peptide linker (FA-RRK(Ce4)-OH) as shown in Fig. 1B. The di-arginine (RR) residues in the linker are a well-known substrate of lysosomal cathepsin B.[7] Numerous studies have shown that cathepsin B overexpression is correlated with invasive and metastatic cancers as well as poor therapy outcome.[8] Therefore, this dual-targeted FA-photosensitizer conjugate may enable NIR fluorescence imaging of FAR-positive and cathepsin B-overexpressing cancer cells with a high target-to-background ratio and the selective PDT of target cells without side effects.

FRC conjugates were synthesized by 9-fluorenylmethoxycarbonyl solid phase peptide synthesis (Fmoc SPPS) using ASP48S, and purified by the reverse phase high performance liquid chromatography. Molecular weights of the purified FRC conjugates were confirmed using LC/MS (Fig. S1 and S2). The molar mass of the synthesized FRC conjugate was 1,416 g/mol. From analysis of the UV-Vis absorption spectrum of the FRC conjugate, absorption peaks assigned to FA (*i.e.*, peak at 285 nm) and Ce4 (*i.e.*, peaks at 403, 505, and 660 nm) were observed (Fig. 1C and Fig. S3), confirming the successful conjugation of FA and Ce4 to produce the FRC conjugate.

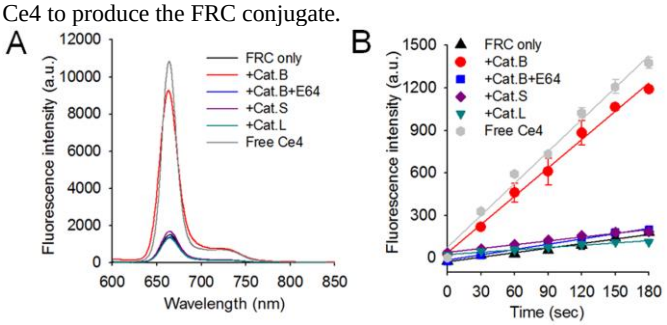

Fig. 2 a) Representative fluorescence spectra of free Ce4, buffer-treated FRC conjugate and FRC conjugates incubated with cathepsin B (Cat. B), E64-pretreated Cat. B, cathepsin S (Cat. S), and cathepsin L(Cat. L) ($\lambda_{ex.}$ 400 nm). b) Time-dependent changes in SOSG fluorescence intensities during 670-nm laser irradiation (n = 4).

We then evaluated the quenching and recovery of the fluorescence and SOG of the FRC conjugate. The FRC conjugate fluorescence emission was quenched under both *in vitro* and *in vivo* conditions. Fig. 1D shows NIR fluorescence images of free Ce4 and FRC conjugate solutions in the microtubes and also at sites of subcutaneous injection in athymic nude mice (Fig. S4). FRC treated with cathepsin B showed a 6-fold increase in fluorescence intensity compared to that of buffer-treated FRC conjugate (Fig. 2A and Fig. S5A). Pretreatment of cathepsin B with its inhibitor (E64) completely inhibited the recovery of the fluorescence of the FRC conjugate upon cathepsin B addition (Fig. 2A). Treatment of the FRC conjugate with other cathepsins (*i.e.*, cathepsin S and L which are lysosomal enzymes with similar arginine selectivity)[9] did not induce any recovery of the fluorescence intensity of the FRC conjugate, confirming that the recovery of the fluorescence was specific to cathepsin B. In parallel to fluorescence experiments, we measured SOG from the FRC conjugate in the absence and presence of cathepsins by using singlet oxygen sensor green (SOSG) as a singlet-oxygen-detecting reagent (Fig. 2B and Fig. S5B). SOSG fluorescence in the cathepsin B-treated FRC conjugate increased significantly with time during 670-nm laser irradiation, whereas SOSG fluorescence in the buffer-treated FRC conjugate control showed a minor increase. In fact, SOG of cathepsin B-treated FRC conjugate was 6.67-fold greater than that of the buffer-treated FRC conjugate control, whereas treatment of FRC conjugates with either E64-pretreated cathepsin B or the other cathepsins did not induce SOG recovery. These results demonstrate that FA within close proximity to Ce4 acts as an efficient quencher of both the fluorescence and SOG of Ce4. Specific cleavage of the peptide linker by cathepsin B caused the release of Ce4 from the conjugate, turning on both the fluorescence emission and SOG of Ce4. To the best of our knowledge, the quenching in the fluorescence and SOG of photosensitizers proximal to FA has never been reported. Because there is no overlap between the fluorescence emission of Ce4 and the excitation wavelength of FA, fluorescence resonance energy transfer (FRET) from Ce4 to FA should be ruled out. One potential mechanism of quenching is photoinduced electron transfer (PET), which is strongly dependent on the distance between an electron donor and acceptor.[10]

Prior to the *in vitro* cell studies, the effects of serum proteins on the fluorescence recovery of the FRC conjugate were examined. The FRC conjugate was dissolved in PBS solution containing 10% fetal bovine serum (FBS) and its fluorescence changes were then monitored for 4 h at 37 ℃ (Fig. S6). As a result, no increase in FRC conjugate fluorescence was observed during the 4 h incubation, indicating that serum proteins do not interfere with the activation of FRC conjugates.

Next, the utility of the FRC conjugate in activatable NIR fluorescence imaging of target cells was tested in *in vitro* cell studies using a live cell imaging system. We applied both free Ce4 and FRC conjugate at 2 μM to FAR-overexpressing KB (human epidermoid carcinoma) cells.[11] Because the NIR fluorescence of the FRC conjugate was expected to be quenched in the extracellular space and turned on only inside target cells, the NIR fluorescence images ($\lambda_{ex.}$ 640 ± 15 nm, $\lambda_{em.}$ 690 ± 25 nm) were acquired every 15 min for 2 h without washing the photosensitizers (Fig. S7). As expected, minor fluorescence signals were detected in both the extracellular and intracellular spaces of FRC-treated cells at the initial time point. Thereafter, FRC-treated cells became brighter with time and were strongly fluorescent after 2 h of incubation, indicating fluorescence recovery of the FRC conjugate inside the cells. In contrast, strong red fluorescence was continuously observed in free Ce4-treated cells over the 2 h period because the fluorescence of free Ce4 is always turned on. This data from the live cell imaging studies confirm the utility of the FRC conjugate in NIR fluorescence imaging of FAR-positive cancers with a high target-to-background ratio. We further corroborated FAR-mediated internalization and subsequent fluorescence activation of the FRC conjugate by using confocal laser scanning microscopy (CLSM). Briefly, KB cells were incubated with 2 μM FRC conjugate or free Ce4 for 4 h. In competition assays, KB cells were incubated with FRC conjugate or free Ce4 in the presence of 1 mM FA. In enzyme inhibition studies, KB cells were incubated with a cell-permeable cathepsin B inhibitor (E64d, 100 μM) for 30 min followed by co-incubation with the FRC conjugate or free Ce4 for an additional 4 h. Untreated control cells were incubated for 4 h in the absence of photosensitizers. All cells were then washed 3 times before fluorescence images of the cells were

obtained ($\lambda_{ex.}$ 405 nm and $\lambda_{em.}$ 625–754 nm). Fig. 3A shows that FRC-treated KB cells were found to be highly fluorescent following 4 h of incubation but they became non-fluorescent when co-treated with free FA (1 mM) as a competitor. In addition, KB cells pretreated with E64d were weakly fluorescent. These results indicate the FAR-mediated intracellular uptake of the FRC conjugate and its subsequent fluorescence activation by intracellular cathepsin B. Interestingly, KB cells treated with free Ce4 were much less fluorescent than FRC-treated cells, indicating the low intracellular uptake of free Ce4 compared to that of the FRC conjugate. Fluorescence intensities from the free Ce4-treated KB cells were not affected by co-incubation with either free FA (1 mM) or E64d. Therefore, these data further confirm that incubation with the FRC conjugate results in enhanced and specific intracellular uptake *via* receptor-mediated endocytosis and release of Ce4 from the FRC conjugate by lysosomal cathepsin B, both of which lead to significantly improved fluorescence intensities compared to that of free Ce4-treated cells. Lysosomal localization of the FRC conjugate was verified by lysosome staining with LysoTracker and co-localization with Ce4 fluorescence are shown in Fig. S8.

To examine cytotoxicity of the FRC conjugate, KB cells were treated with the FRC conjugate over a concentration range of 0–10 μM for 24 h. FRC-treated KB cells showed no cytotoxicity in the absence of light exposure at the tested concentrations (Fig. S9). Next, target-cell-specific and activatable PDT with the FRC conjugate was evaluated (Fig. 3B). KB cells were incubated with FRC conjugate at 5 μM for 4 h, washed 3 times, and then irradiated using a 670-nm laser at a light dose of 20 J/cm^2 (dose rate: 50 mW/cm^2). For competition assays, KB cells were incubated with the FRC conjugate in the presence of 1 mM free FA. For inhibition assays in the inhibitor-treated group, cathepsin B activity was inhibited by treating cells with E64d (100 μM) and the FRC conjugate (Fig. 3B). FRC-treated KB cells exhibited 62% cell death upon light irradiation. Co-incubation with free FA resulted in a negligible PDT effect owing to the prevention of the FRC binding to FAR on the cell surface of KB cells. Inhibition of cathepsin B activity in KB cells also resulted in a marked reduction in the phototoxic effect, as cell viability in the inhibitor-treated group was slightly lower than that in the free FA-treated group. This observation could be attributed to the fact that co-incubation with free FA prevented the FRC conjugate uptake into KB cells, whereas E64d only inhibited the activation of FRC conjugate internalized into the cells. These results confirm that the PDT effect of the FRC conjugate is switched on inside cells after specific internalization of FRC conjugate into FAR-positive cancer cells.

Next, we used a xenografted mouse model to assess the utility of the FRC conjugate for *in vivo* fluorescence imaging and PDT. The KB cell lines were subcutaneously implanted into the hind flank of each mouse, and tumors were allowed to grow to approximately 50 mm^3. Following tail vein injection with PBS (100 μL/mouse), free Ce4 (1 mg/kg), and the FRC conjugate (1 mg Ce4 eq./kg), NIR fluorescence images were obtained at 3 h, 5 h, and 24 h after injection, respectively (Fig. S10A and Fig. 4A). Strong fluorescence signals were observed in tumors of FRC treated mice, indicating the accumulation of the FRC conjugate in the FAR-positive tumor tissues and subsequent activation of its fluorescence. High fluorescence intensities at tumor sites were maintained until 24 h after injection, clearly discriminating the tumors from surrounding normal tissues. Tumor-to-background ratio in the FRC-treated mice were 5.2±0.9 (Fig. S10B). In contrast, no significant fluorescence signals were observed in tumors and surrounding normal tissues of free Ce4-treated mice. High fluorescence signals shown in the intestine region of free Ce4-treated mice at 3 h post-injection (Fig. S10A) suggest that most of the hydrophobic free Ce4s were rapidly eliminated from the blood circulation *via* hepatobiliary excretion as shown in Fig. S11.

To investigate therapeutic efficacy *in vivo*, PBS, free Ce4, or FRC conjugate was injected intravenously. After 24 h, tumors were illuminated with a 670-nm CW laser at a light dose of 30 J/cm^2 (dose rate = 100 mW/cm^2). Remarkably, enhanced *in vivo* therapeutic effect was observed in the FRC-treated group compared with that in the free Ce4-treated group. In the group that received FRC conjugate with light illumination, the mean tumor volume was 53% at day 8 (P < 0.05) compared to that of the control group (Fig. 4B). The mean tumor volume in the free Ce4-treated group with light illumination showed 83% at day 8 compared to that of the

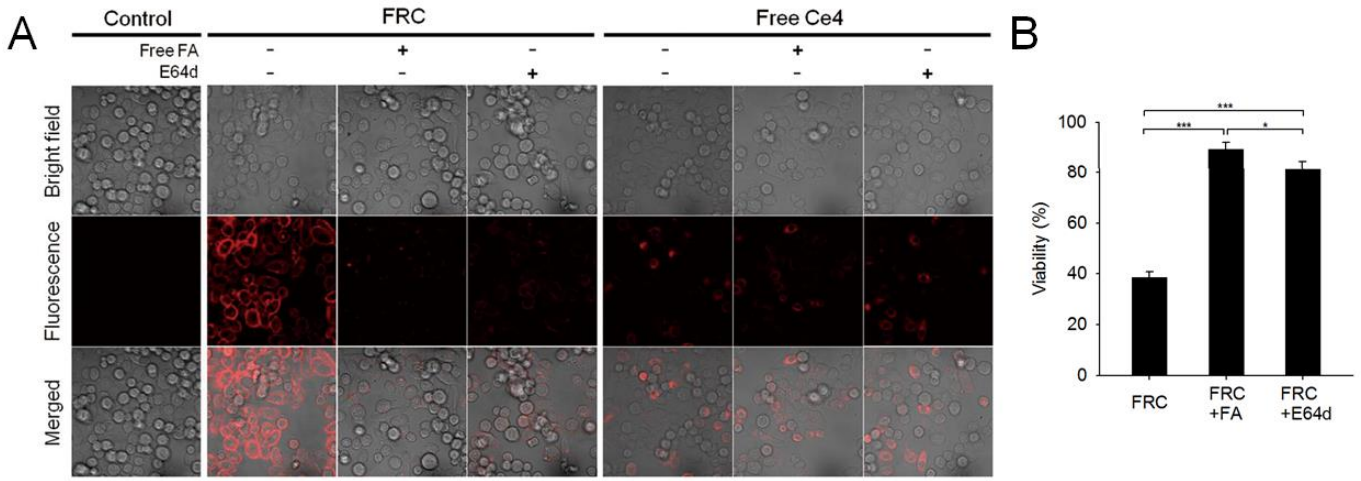

Fig. 3 a) Confocal fluorescence images of KB cells treated with the FRC conjugate and free Ce4 for 4 h at various conditions. Free FA (1 mM) was co-incubated with the photosensitizers to prohibit the FRC conjugate binding to FARs. Cell-permeable cathepsin B inhibitor, E64d (100 μM), was applied to cells to inhibit cathepsin B activity in KB cells. Untreated control cells were incubated without photosensitizers. (b) *In vitro* photodynamic efficacy of the FRC conjugate. KB cells were treated with the FRC conjugate at 5 μM with or without free FA (1 mM) for 4 h followed by irradiation with a 670-nm CW laser (50 mW/cm^2, 20 J/cm^2). E64d (100 μM) was applied to inhibit cathepsin B activity inside KB cells. *, P < 0.05; **, P < 0.01; and ***, P < 0.001.

control group (P = 0.46).

No significant difference in body weight was observed between groups at day 8 (Fig. S12).

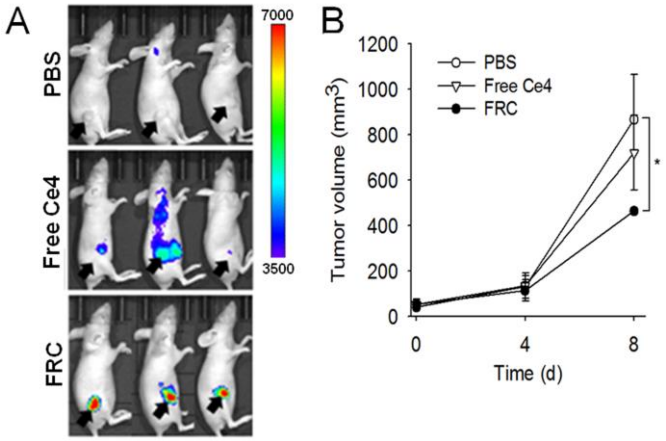

Fig. 4 a) NIR fluorescence images of the PBS, FRC-treated, and free Ce4-treated mice were obtained 24 h after injection ($\lambda_{ex.}$ 660 ± 10 nm, $\lambda_{em.}$ 710 ± 20 nm). The arrows indicate tumor sites. b) *In vivo* PDT. PBS + PDT (n = 5); FRC + PDT (n = 3); free Ce4 + PDT (n = 3). *, P < 0.05.

In summary, results in both *in vitro* cell and *in vivo* animal studies verified that the folate-photosensitizer conjugate linked *via* cleavable bonds is useful for dual-targeted NIR fluorescence imaging and PDT of cancer cells with high specificity.

This work was supported by a National Cancer Center grant (1310160 and 1410676), Republic of Korea.

Notes and references

[a] Molecular Imaging & Therapy Branch, National Cancer Center, 323 Ilsan-ro, Goyang-si, Gyeonggi-do 410-769, Korea. E-mail: ydchoi@ncc.re.kr; Fax: +82-31-920-2529; Tel: +82-31-920-2512
[b] Molecular Imaging Innovations Institute, Department of Radiology, Weil Cornell Medical College, New York, NY 10065, United States.
† Electronic Supplementary Information (ESI) available: See DOI: 10.1039/c000000x/

1 D. E. Dolmans, D. Fukumura and R. K. Jain, *Nat. Rev. Cancer*, 2003, **3**, 380.
2 Y. N. Konan, R. Gurny and E. Allemann, *J. Photochem. Photobiol. B*, 2002, **66**, 89.
3 (*a*) K. Stefflova, H. Li, J. Chen and G. Zheng, *Bioconjugate Chem.*, 2007, **18**, 379; (*b*) A. M. Bugaj, *Photochem. Photobiol. Sci.*, 2011, **10**, 1097; (*c*) S. Wang, J. Wang and J. Y. Chen, *J. Mater. Chem. B*, 2014, **2**, 1594.
4 (a) J. Gravier, R. Schneider, C. Frochot, T. Bastogne, F. Schmitt, J. Didelon, F. Guillemin and M. Barberi-Heyob, *J. Med. Chem.*, 2008, **51**, 3867; (*b*) D. Li, P. Li, H. Lin, Z. Jiang, L. Guo and B. Li, *J. Photochem. Photobiol.*, 2013, **127**, 28; (*c*) B. Chen, B. W. Poque, P. J. Hoopes and T. Hasan, *Crit. Rev. Eukaryot. Gene Expr.*, 2006, **16**, 279.
5 (*a*) J. M. Saul, A. Annapragada, J. V. Natarajan and R. V. Bellamkonda, *J. Control. Release*, 2003, **92**, 49; (*b*) K. B. Ghaghada, J. Saul, J. V. Natarajan, R. V. Bellamkonda and A. V. Annapragada, *J. Control. Release*, 2005, **104**, 113.
6 P. S. Low, W. A. Henne and D. D. Doorneweerd, *Acc. Chem. Res.*, 2008, **41**, 120.
7 (*a*) K. I. Hulkower, C. C. Butler, B. E. Linebaugh, J. L. Klaus, D. Keppler, V. L. Giranda and B. F. Sloane, *Eur. J. Biochem.*, 2000, **267**, 4165; (*b*) A. J. Barrett, *Anal. Biochem.*, 1976, **76**, 374. (c) A. J. Barrett, *Biochem. J.*, 1980, **187**, 909.
8 (*a*) C. S. Gondi and J. S. Rao, *Expert Opin. Ther. Targets*, 2013, **17**, 281; (*b*) R. Frlan and S. Gobec, *Curr. Med. Chem.*, 2006, **13**, 2309.
9 A. J. Barrett and H. Kirschke, *Methods Enzymol.*, 1981, **80**, 535.
10 (a) H. Lee, J. Kim, H. Kim, Y. Kim and Y. Choi, *Chem. Commun.*, 2014, **50**, 7507; (b) S. Doose, H. Neuweiler and M. Sauer, *ChemPhysChem* 2009, **10**, 1389.
11 A. L. Jackman, D. S. Theti and D. D. Gibbs, *Adv. Drug Deliv. Rev.*, 2004, **56**, 1111.